Comparison of finite-difference and ray-theory seismograms in the elastic SEG/EAGE Salt Model, shot number 145

Václav Bucha
Department of Geophysics, Faculty of Mathematics and Physics, Charles University, Ke Karlovu 3, 121 16 Praha 2, Czech Republic, E-mail: bucha@seis.karlov.mff.cuni.cz

Summary

Finite-difference seismograms for a selected shot and two receiver configurations computed in the elastic SEG/EAGE Salt Model during the Next-Generation Seismic Modeling and Imaging project are compared with ray-theory seismograms calculated using the SW3D software. Two-point rays of direct, refracted and reflected P-waves and converted S-waves in the smoothed elastic SEG/EAGE Salt Model are computed.

Keywords

Elastic velocity model, ray tracing, seismic waves, synthetic seismograms

1 Introduction

The original acoustic SEG/EAGE Salt Model contains P-wave velocity values (Aminzadeh *et al.*, 1997). House *et al.* (2004) calculated finite-difference seismograms in an elastic SEG/EAGE Salt Model. This elastic velocity model was supplemented by values of S-wave velocities and densities derived from the original P-wave velocity values. Elastic wave calculations were carried out using the modeling program called "E3D" (Larsen and Grieger, 1998). E3D is a finite-difference modeling code (4th order accurate in space, and 2nd order in time).

House *et al.* (2004) performed elastic numerical calculations within the Next-Generation Seismic Modeling and Imaging project. The project started in 2000, as a colaboration among 20 industry companies, two US national laboratories (Los Alamos National Laboratory and Lawrence National Laboratory), two universities (Stanford University and the University of Houston), and the modeling subcommittee of the SEG Research Committee. SEGY synthetic seismograms computed within Phase 1 finite-difference calculations in the elastic SEG/EAGE model are available via internet (http:// www.ees11.lanl.gov/projects/next-gen).

We compared finite-difference seismograms for shot number 145 and two receiver configurations, marine streamers and ocean bottom cables, with ray-theory seismograms of selected elementary waves computed using the SW3D software. Smoothed SEG/EAGE Salt Model (Bulant, 2001, 2002, 2003) supplemented by S-waves and densities was used for ray tracing calculations.

Programs and data files referred in this paper and used for computation are included on compact disk SW3D-CD-9 (Bucha & Bulant, 2005) in packages CRT, MODEL, FORMS and DATA. The GOCAD program was used for visualization of the 3-D smoothed Salt Model interfaces, shot, receiver configurations and computed rays. The

In: Seismic Waves in Complex 3-D Structures, Report 15 (Department of Geophysics, Charles University, Prague, 2005), pp. 189–206

figures in the paper are GOCAD screen snapshots of limited resolution. All computations were performed on a PC equipped with Athlon XP 2400+ (2GHz) processor and with RedHat Linux operating system.

2 Elastic smoothed SEG/EAGE Salt Model

The smoothed SEG/EAGE Salt Model (Bulant, 2001, 2002, 2003) with the most important interfaces (ocean bottom, interfaces limiting the salt body, geopressure horizon, bottom flat interface, see Figure 1) derived from the original acoustic model (Aminzadeh *et al.*, 1997) was supplemented by S-waves and densities according to House *et al.* (2000). S-wave velocities were derived from the smoothed P-wave velocities with a piecewise linear dependence of ratio V_p/V_s on the depth (Table 1). Densities in sediments were derived from P-wave velocities using the Gardner relation (Gardner *et al.*, 1974),

$$\varrho = 0.23 * (V_p)^{1/4} \quad ,$$

where ϱ is density (g/cm^3) and V_p is P-wave velocity (Ft/s). Constant density of 2.2g/cm^3 was used for salt.

Depth (km)	V_p/V_s
Water (all depths)	∞ ($V_s = 0.0$)
0.0 sediments	5.0
0.6	3.5
1.5	3.0
3.0	2.5
4.5	2.3
6.0	2.0
Salt (all depths)	1.9

Table 1. V_p/V_s values that approximates a velocity depth trend appropriate for the Gulf of Mexico.

Gridded data for six surfaces and five complex blocks (P and S wave slownesses and densities) of the elastic smoothed SEG/EAGE Salt Model are specified in the file `sal-mod3.dat`.

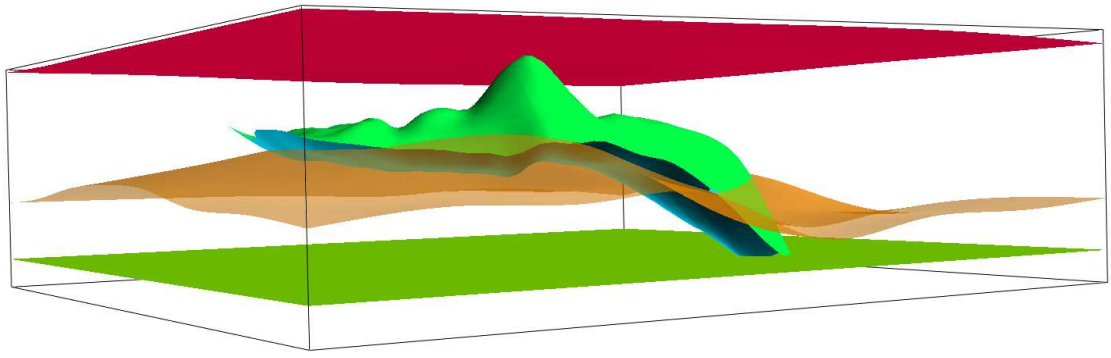

Figure 1. Smoothed Salt Model with the most important interfaces, ocean bottom (red), interfaces limiting the salt body (green and blue), geopressure horizon (brown), bottom flat interface (green). Interfaces are coloured according to the indices of surfaces. The geopressure horizon is partially transparent.

3 Source and receivers

Ray tracing computations were performed for one shot common for two receiver configurations, marine streamers and ocean bottom cables. The shot corresponds to shot number 145 in the Next Generation Seismic Modeling and Imaging project, Phase 1 where a 17 by 17 grid of shot locations was defined, with a shot spacing of 480 m (House *et al.*, 2004). The grid of shots covers almost the entire salt body of the SEG/EAGE model. The selected shot number 145 is located at the center of the grid.

Figure 2 shows the location of the selected shot and eight receiver lines above the salt body. The shot (magenta point) is located in the ocean in the depth of 12m. The eight black lines represent marine streamers. Each line consists of 141 groups of one-component hydrophones with a group interval of 24m. Hydrophones are located in the depth of 12m. The name and coordinates of the shot are in file `s145-src.dat`. The names and coordinates of the marine receivers are in eight files `s145se1r.dat`,...,`s145se8r.dat`. Numbers of receiver lines are denoted by numbers 1,...,8 from the right-hand side to the left-hand side in the Figure 2.

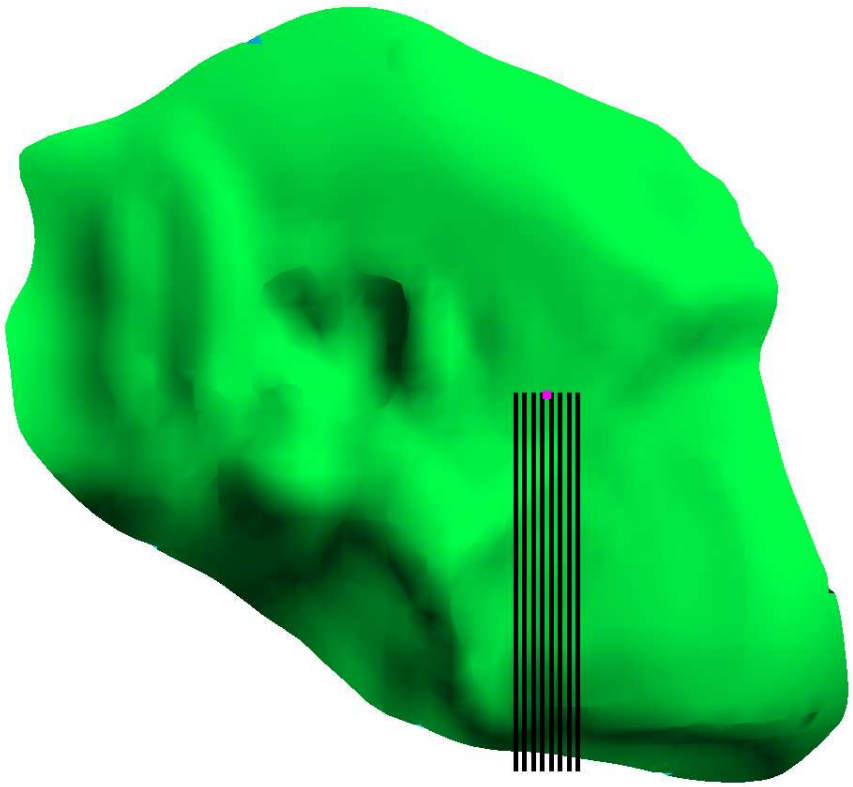

Figure 2. Top view of the shot, eight receiver lines and salt body. Magenta point represents the source in the depth of 12m. Black lines represent marine receivers in the depth of 12m.

Figure 3 shows the location of the selected shot (magenta point) and six receiver lines above the salt body. The six black lines represent four component ocean bottom cables. Each line consists of 281 groups with a group interval of 24m. Each receiver group contains a hydrophone as well as a three-component set of geophones (House *et al.*, 2000). The names and coordinates of the ocean bottom cable receivers are in files

`s145oe1r.dat`,...,`s145oe6r.dat`. Hydrophones and geophones are located at the ocean bottom interface and program `intf.for` was used to calculate correct depths. Numbers of receiver lines are denoted by numbers 1,...,6 from the right-hand side to the left-hand side in the Figure 3.

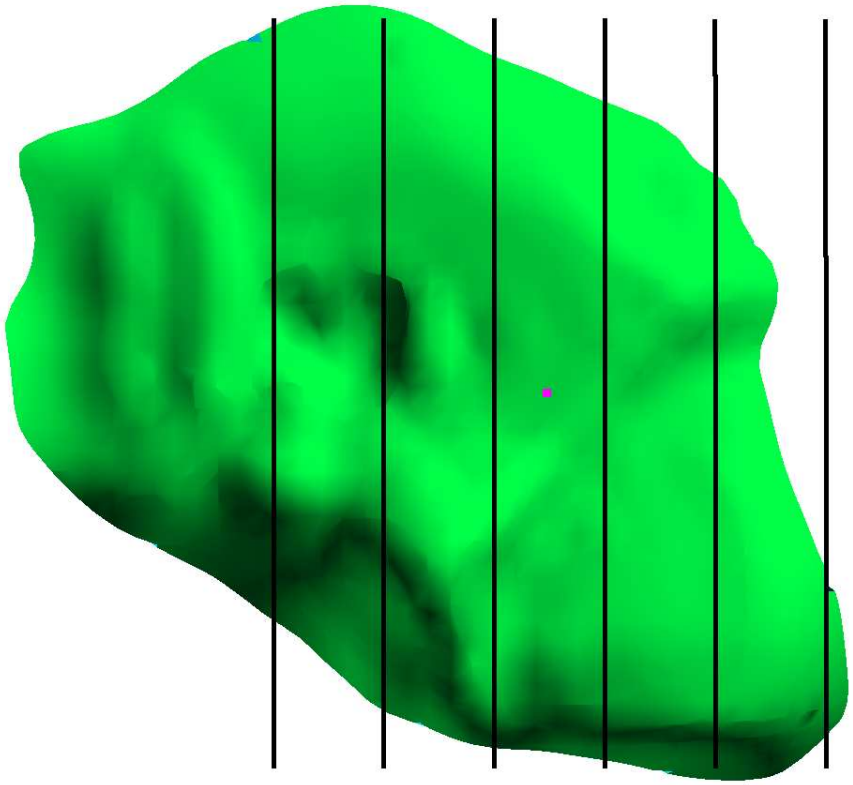

Figure 3. Top view of the shot, six receiver lines and salt body. Violet point represents the source in the depth of 12m. Black lines represent ocean bottom cable receivers.

4 Ray tracing computations

Computation of rays and synthetic seismograms in the elastic smoothed SEG/EAGE Salt Model was performed using the SW3D software. The history files manage the computation of rays, seismograms and generate PostScript and GOCAD files for visualization. Detailed description of the use of history files can be found in older report papers, e.g., Bulant & Klimeš (1998), Bucha (2001). In this paper only short description of the computation steps will be presented.

Two–parametric shooting method is used for two–point ray tracing. Program `crtray.for` converts the unformatted output of program `crt.for` into formatted files with rays suitable for plotting. Program `linwrl.for` writes rays of computed waves into GOCAD files. Program `ptswrl.for` does the same for the shot and receivers. Figures 4, 5, 6, 7, 8 and 9 show rays of computed waves. The figures are screen snapshots of several GOCAD camera positions with limited resolution. Some interfaces are partially transparent.

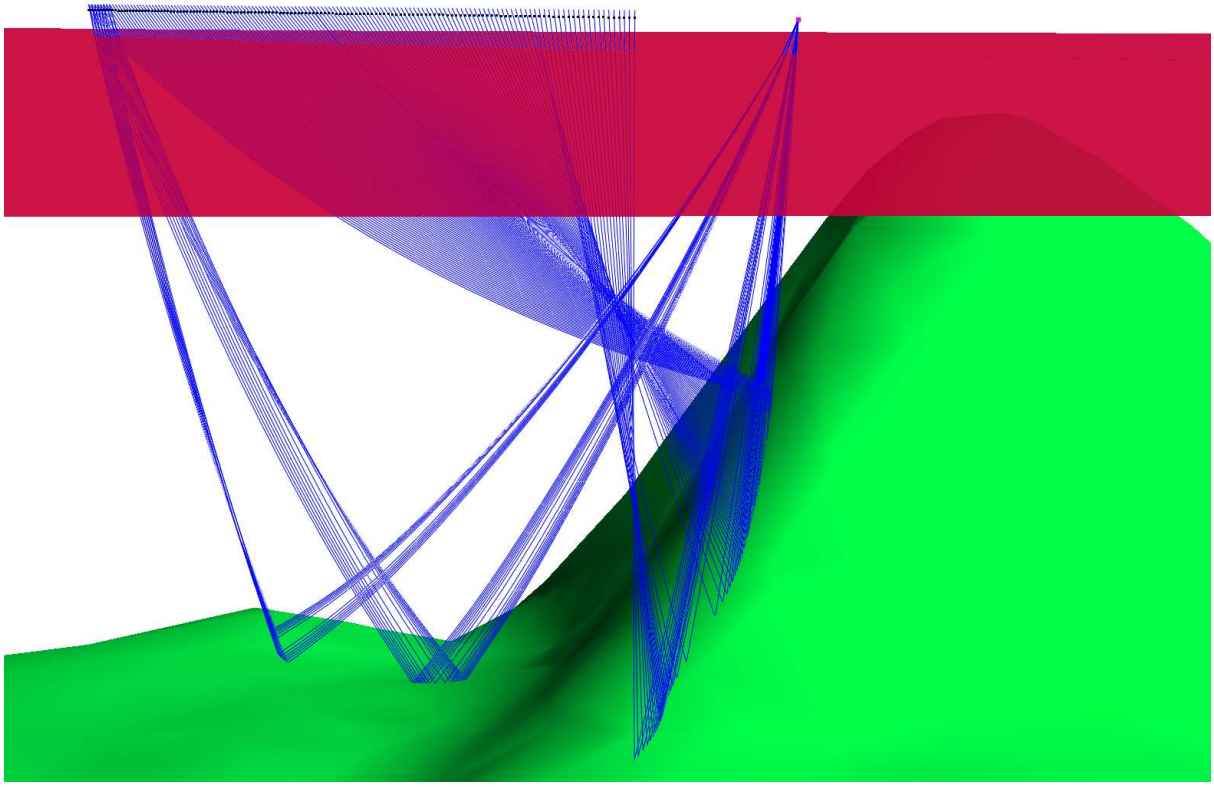

Figure 4. Rays of P-wave reflected from the salt top interface (marine receiver line 1). The ocean bottom interface is partially transparent.

4.1 Marine configuration

History files `s145se1.h`,...,`s145se8.h` summarize parameters and execute programs that calculate simulation of marine survey for one shot and eight receiver lines (each history file computes rays and seismograms for the shot and one receiver line). Two-point rays of 24 elementary waves were calculated.

(1) 18 elementary P-waves: direct wave, wave refracted under the ocean bottom, wave refracted in the salt body, 1x, 2x, 3x, 5x, 10x reflected from the ocean bottom, combinations of wave refracted under the ocean bottom and reflected from the ocean bottom, wave reflected 1x and 2x from the top of salt body, wave reflected from the bottom of the salt body, wave reflected from the bottom interface.

(2) 6 elementary P-waves converted to S-waves and back to P-waves: P-wave reflected and converted to S-wave at the top of the salt body, P-wave refracted and converted to S-wave in the salt body, P-wave reflected and converted to S-wave at the bottom of the salt body, P-wave converted to S-wave at the top of the salt body and reflected from the bottom of the salt body, P-wave converted to S-wave at the bottom ocean interface and reflected from the top of the salt body, P-wave converted to S-wave at the bottom ocean interface and reflected from the bottom of the salt body.

Top interface (sea level) at the depth of 0m is used for storing computed quantities. Receivers are in the depth of 12m and travel times are interpolated from the top interface. Following files are common for all eight history files. The codes of elementary waves are defined in the file `se-cod1.dat`. Data specifying the take-off parameters of the required rays are specified in the file `se-rpa1.dat`. The input data for the complete ray tracing

are stored in the file `se-dcr1.dat`. The file `se-wri1.dat` specifies the names of the output files with the computed quantities.

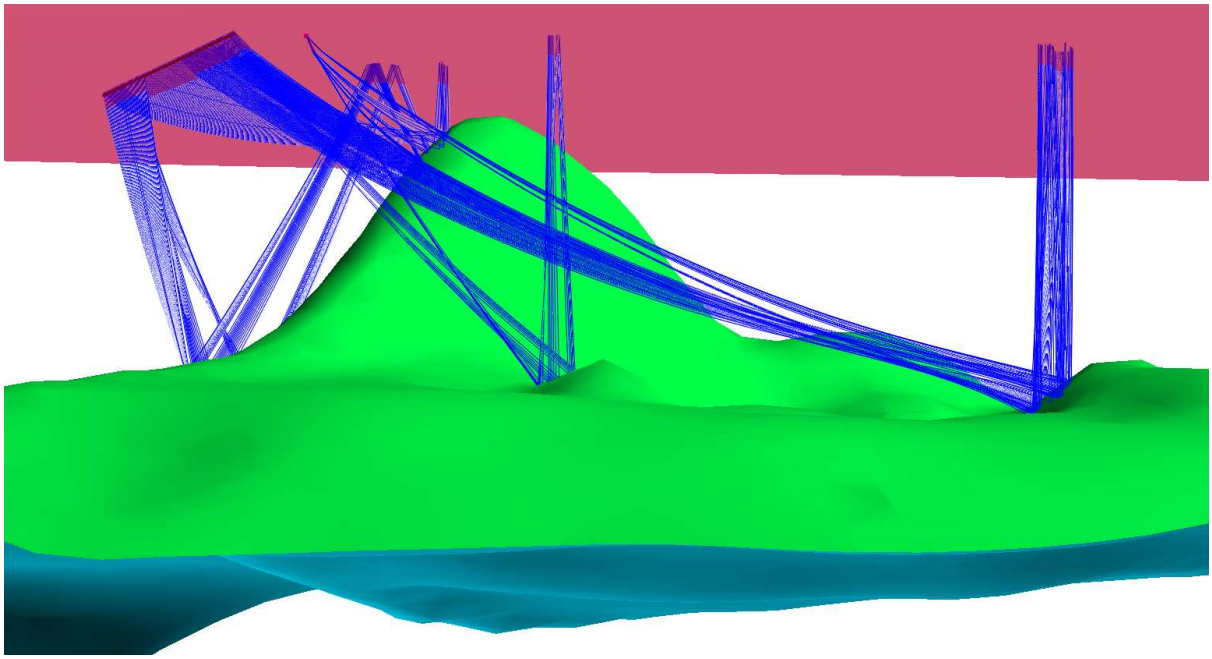

Figure 5. Rays of P-wave 2x reflected from the salt top interface and reflected from the sea level (marine receiver line 1). The ocean bottom interface is partially transparent.

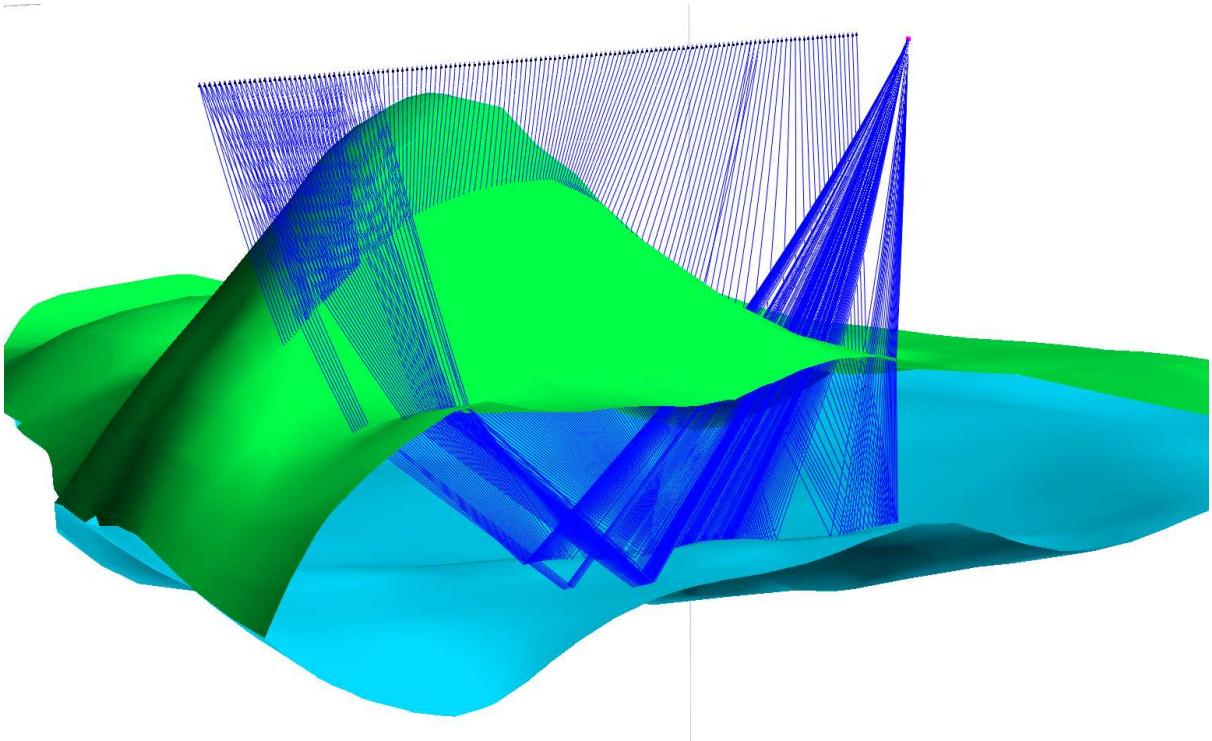

Figure 6. Rays of P-wave reflected from the salt bottom interface (marine receiver line 8). The model is cut by GOCAD slicer.

4.2 Ocean bottom cable configuration

History files `s145oe1.h`,...,`s145oe6.h` summarize parameters and execute programs that calculate simulation of ocean bottom cable survey for one shot and six receiver lines.

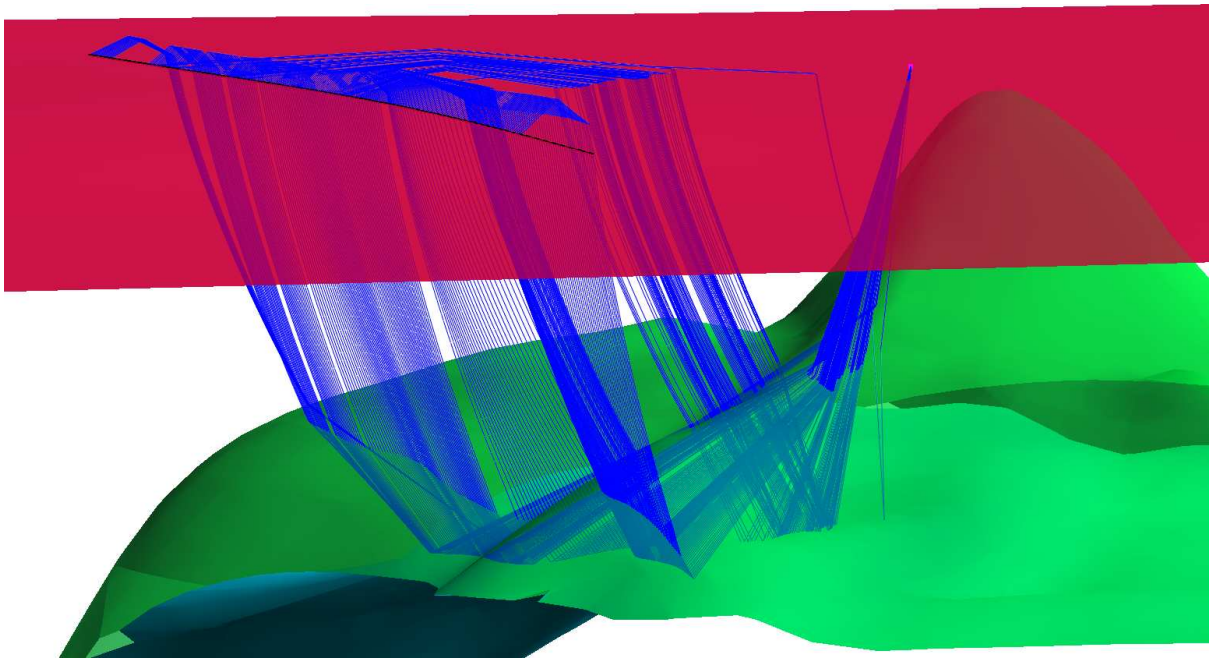

Figure 7. P-wave reflected and converted to S-wave at the bottom of the salt body and reflected from the sea level (ocean bottom cable line 1). The ocean bottom interface and salt top interface are partially transparent.

Two-point rays of 30 elementary waves were calculated.

(1) During the computations of direct P-wave some of the rays were tangent to the weakly curved ocean bottom surface and the computation crashed. The position of receivers is at the ocean bottom. It was necessary to add reference surface near to the ocean bottom, and to project all receiver points onto the reference points "visible" to rays. The travel times were extrapolated from the reference points to the receivers. Code for elementary direct P-wave is defined in the file `oe-cod1a.dat`, data specifying the take-off parameters in the file `oe-rpa1a.dat` and data for complete ray tracing in the file `oe-dcr1a.dat`.

(2) 16 elementary waves were stored at the positive ("top") side of the ocean bottom surface. The last reflection before storing was from the sea level. Codes for 16 elementary waves are defined in the file `oe-cod1b.dat`.

(2a) 11 elementary P-waves: 1x, 2x, 4x, 9x reflected from the ocean bottom, combinations of wave refracted under the ocean bottom and reflected from the ocean bottom, wave reflected 1x and 2x from the top of salt body, wave reflected from the bottom of the salt body, wave reflected from the bottom interface.

(2b) 5 elementary P-waves converted to S-waves and back to P-waves: P-wave reflected and converted to S-wave at the top of the salt body, P-wave reflected and converted to S-wave at the bottom of the salt body, P-wave converted to S-wave at the top of the salt body and reflected from the bottom of the salt body, P-wave converted to S-wave at the bottom ocean interface and reflected from the top of the salt body, P-wave converted to S-wave at the bottom ocean interface and reflected from the bottom of the salt body.

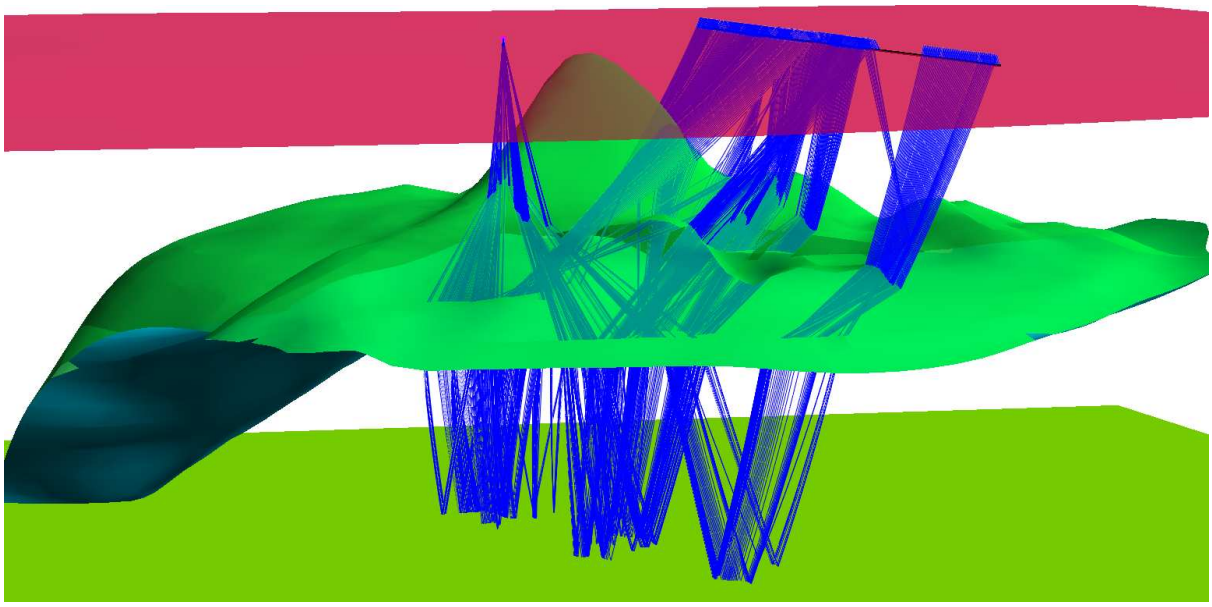

Figure 8. P-wave reflected from the bottom interface and reflected from the sea level (ocean bottom cable line 6). The ocean bottom interface and salt top interface are partially transparent.

Data specifying the take-off parameters are stored in the file `oe-rpa1b.dat` and data for complete ray tracing in the file `oe-dcr1b.dat`.

(3) 13 elementary waves were stored at the negative ("bottom") side of the ocean bottom surface. Codes for 13 elementary waves are defined in the file `oe-cod1c.dat`.

(3a) 8 elementary P-waves: wave refracted under the ocean bottom, wave refracted in the salt body, combinations of wave refracted under the ocean bottom and reflected from the ocean bottom, wave reflected 1x and 2x from the top of salt body, wave reflected from the bottom of the salt body, wave reflected from the bottom interface.

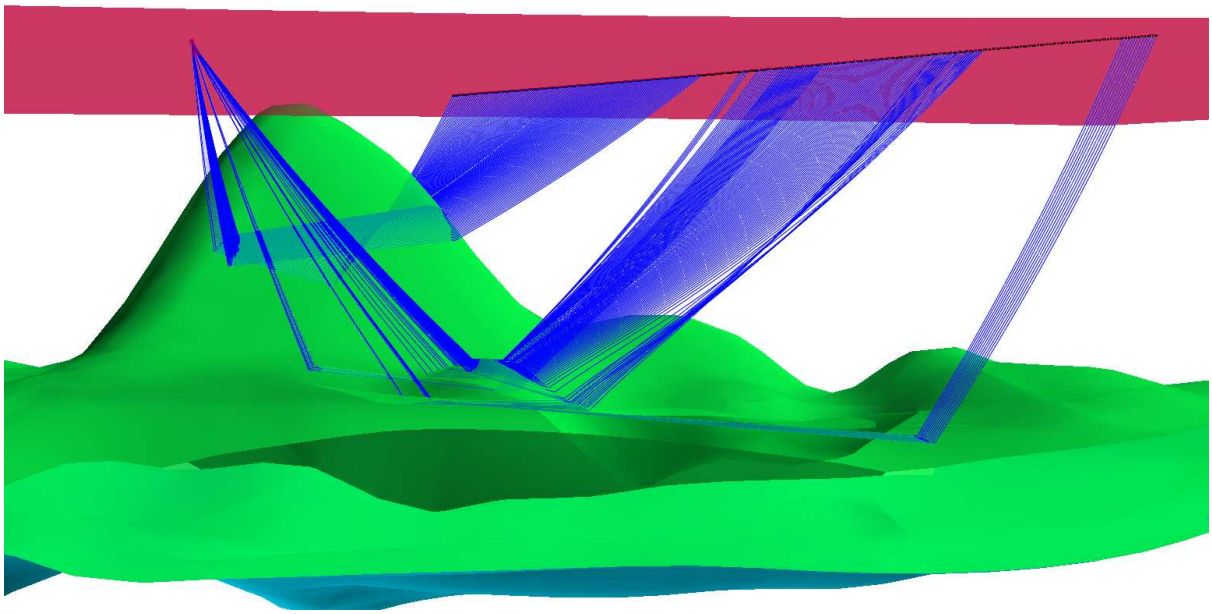

Figure 9. P-wave refracted in the salt body (ocean bottom cable line 6). The ocean bottom interface and salt top interface are partially transparent.

(3b) 5 elementary P-waves converted to S-waves: P-wave reflected and converted to S-wave at the top of the salt body, P-wave reflected and converted to S-wave at the bottom of the salt body, P-wave converted to S-wave at the top of the salt body and reflected from the bottom of the salt body, P-wave converted to S-wave at the bottom ocean interface and reflected from the top of the salt body, P-wave converted to S-wave at the bottom ocean interface and reflected from the bottom of the salt body.

Data specifying the take-off parameters are stored in the file `oe-rpa1c.dat` and data for complete ray tracing in the file `oe-dcr1c.dat`.

The file `oe-wri1.dat` specifies the names of the output files with the computed quantities and is common for all six history files.

5 Comparison of synthetic seismograms

Finite-difference seismograms are read and plotted using the Seismic Unix programs `suswapbytes`, `supswigp` and `psbbox` (Cohen & Stockwell, 2004). The commands and parameters used for figures in the paper are in files `sefdsu.sh` for marine streamers and `oefdsu.sh` for ocean bottom cables. Plots of finite-difference seismograms correspond to hydrophones for marine survey and to vertical component for ocean bottom cable survey. Shots are simulated by air-gun sources, and use a Ricker wavelet with central frequency of 8Hz (House *et al.*, 2004). This frequency represents a compromise between frequency and the amount of computing time required. It seems from the seismograms and frequency analysis that marine streamer survey used 15Hz central frequency source. According to House *et al.* (2000) one shot was also run with a 15Hz central frequency source, maybe shot 145. Seismograms are computed up to the 5s.

Ray-theory seismograms in the frequency domain were computed for eight marine receiver lines and six ocean bottom cable receiver lines. The source time function is defined by the Ricker signal of prevailing frequency 8Hz and 15Hz. The source is an isotropic explosion. Seismograms are computed up to the 8s but plotted only up to the 5s for comparison with finite-difference seismograms. The output of program `crt.for` is converted to the elementary Green functions using program `green.for`. Frequency-domain response function is calculated by program `greenss.for`. The synthetic seismograms are then computed by program `ss.for`.

Plotting of ray-theory seismograms was performed in two ways. Seismograms generated from all the computed elementary waves are at first converted from GSE format to SEGY format by program `gse2segy.for`, read and plotted using the Seismic Unix programs `segyread`, `supswigp` and `psbbox` for better comparison with finite-difference seismograms. The maximum amplitude at each trace is scaled to a given constant. The commands and parameters used for figures in the paper are in files `se1rtsu.sh`,...,`se8rtsu.sh` for marine streamers and `oe1rtsu.sh`,...,`oe6rtsu.sh` for ocean bottom cables.

Seismograms of individual elementary waves distinguished by colours are plotted by program `sp.for`. The maximum amplitude of each elementary wave is scaled to a given constant. Plots of ray-theory seismograms correspond to the vertical component.

Figure 10 shows four plots of marine streamer line 1 synthetic seismograms,
a. Finite-difference seismograms, **b.** Ray-theory seismograms generated from all 24 computed elementary waves. The maximum amplitude at each trace is scaled to a given

constant. The Ricker signal had prevailing frequency 8Hz, **c.** Ray-theory seismograms generated from all 24 computed elementary waves. The Ricker signal had prevailing frequency 15Hz, **d.** Ray-theory seismograms of individual elementary waves distinguished by colours. The maximum amplitude of each elementary wave is scaled to a given constant. The **black** colour denotes direct wave, wave refracted under the ocean bottom, wave refracted in the salt body, **red** denotes multiple reflections from the ocean bottom, **green** denotes combinations of wave refracted under the ocean bottom and reflected from the ocean bottom, **blue** denotes multiple reflections from the top of the salt body, **yellow** denotes wave reflected from the bottom of the salt body, **cyan** denotes wave reflected from the bottom interface, **magenta** denotes P-waves converted to S-waves and back to P-waves. For detailed description see paragraph 4.1. Other marine streamer lines are not plotted because the distance between lines is 80m and the seismograms are similar.

The distance between ocean bottom cable lines is 996m and the differences between seismograms for each line seem to be interesting. That is why seismograms of all six ocean bottom cable lines are presented in the paper. Ray-theory seismograms are generated from 30 computed elementary waves and for detailed description see paragraph 4.2. Figures 11-16 have the same distribution of four plots and use the same colors for elementary waves as Figure 10. The number of ocean bottom cable receivers is twice more than marine streamer receivers and it caused that Figures 11-16 are plotted in lower quality.

Comparison of finite-difference and ray-theory seismograms in this paper show differences. Some of the arrivals of elementary waves are clearly visible on both types of seismograms, some arrivals are not so clear or are shifted in time or position. The differences can be explained by the following facts:

- ray-theory seismograms were computed in the smoothed elastic SEG/EAGE Salt Model,
- amplitudes of ray-theory seismograms are not correct (conversion coefficients are not considered),
- different application of the source time function, Ricker signal (the travel times of the first wave differ),
- ray-theory seismograms are computed for limited number of elementary waves.

Detailed study of the seismograms requires to interactively display rays of elementary waves. The raypaths are for some waves very complicated.

5 Conclusions

Results of this paper demonstrate successful application of the SW3D software to two-point ray tracing and to calculation of ray-theory seismograms in the smoothed elastic Salt Model with interfaces. The paper shows and explains some differences between finite-difference and ray-theory seismograms for shot number 145 and two receiver configurations. Speed, low memory requirements, computation and visualization of raypaths and seismograms of individual elementary waves are great advantages of the ray tracing method.

The time of the computation of the seismograms for one receiver line differs according to position in the model. The time for one marine streamer line was approximately ten hours and for one ocean bottom cable line approximately twelve hours on a PC equipped with processor Athlon XP 2400+ (2GHz).

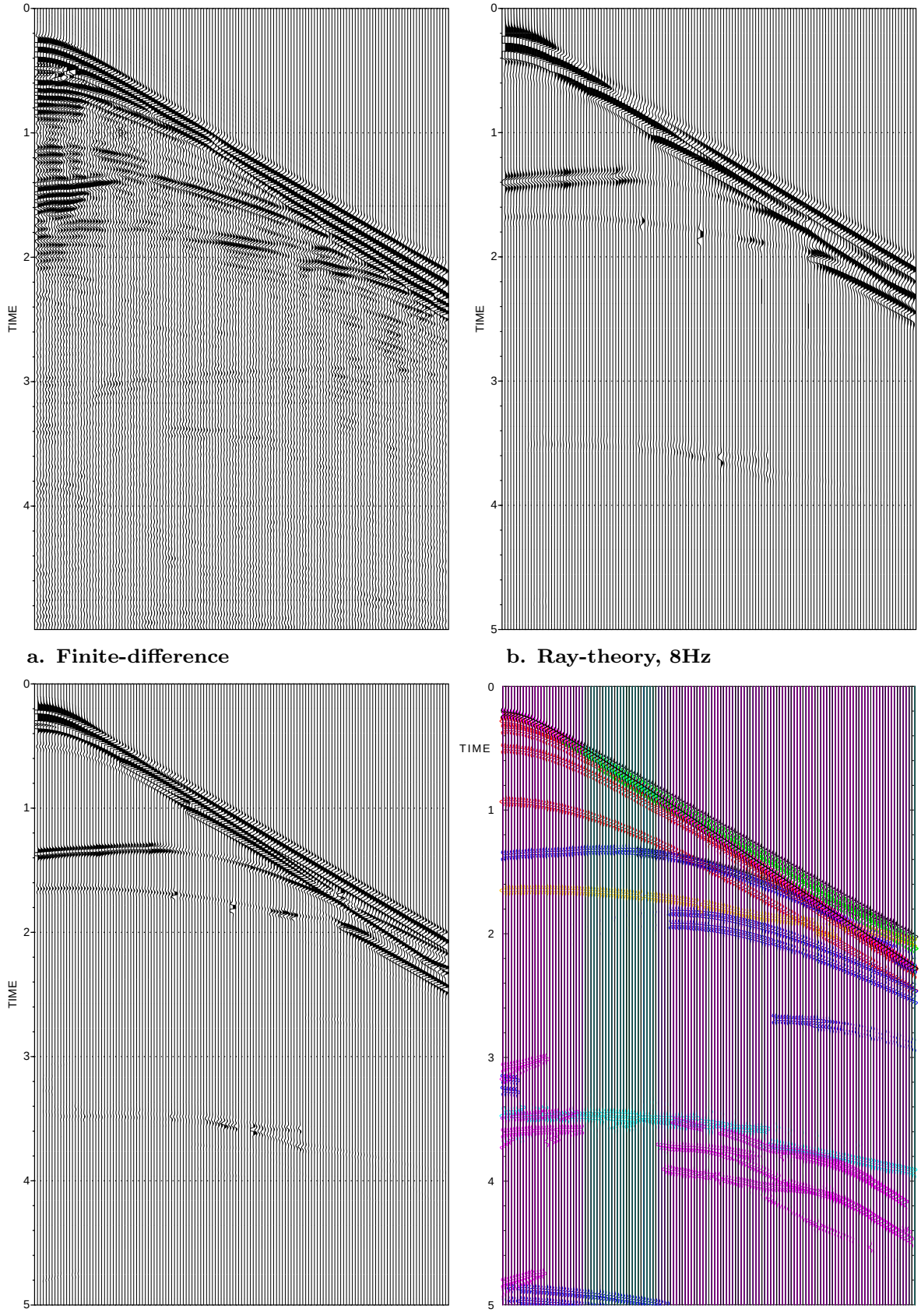

a. Finite-difference **b. Ray-theory, 8Hz**

c. Ray-theory, 15Hz **d. Ray-theory, individual waves, 15Hz**

Figure 10. Marine streamer line 1 seismograms.

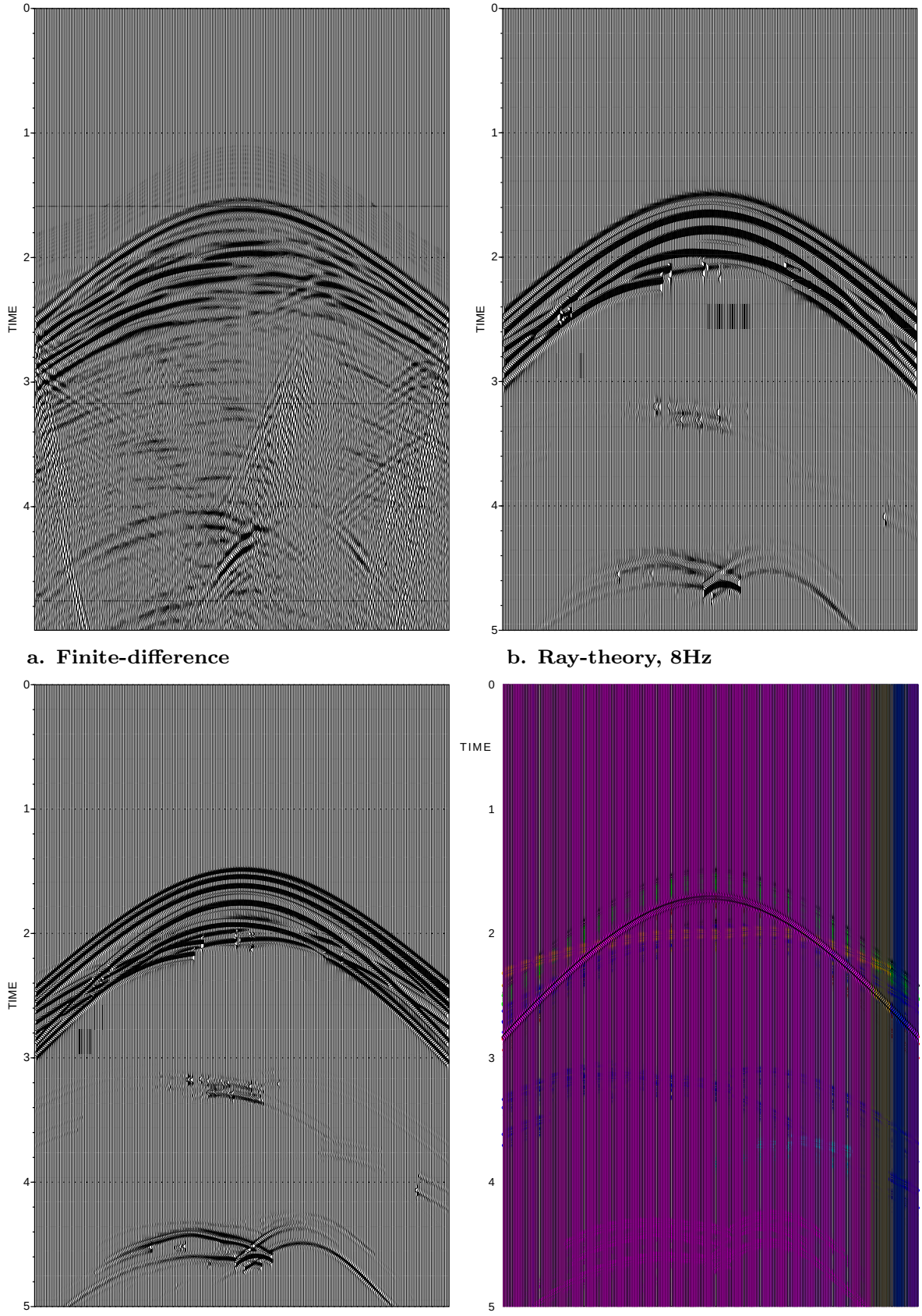

a. Finite-difference **b. Ray-theory, 8Hz**

c. Ray-theory, 15Hz **d. Ray-theory, individual waves, 15Hz**

Figure 11. Ocean bottom cable line 1 seismograms.

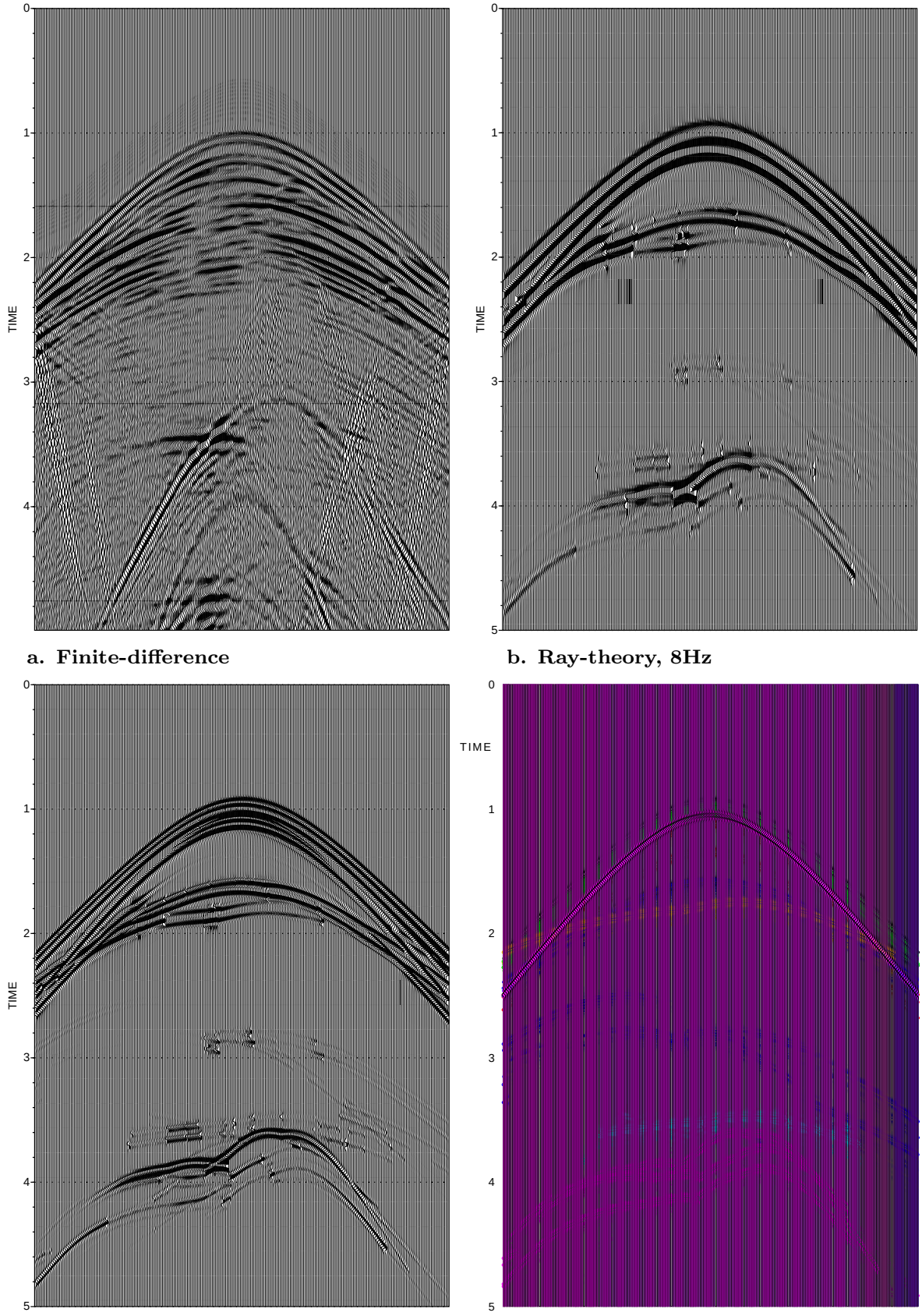

a. Finite-difference **b. Ray-theory, 8Hz**

c. Ray-theory, 15Hz **d. Ray-theory, individual waves, 15Hz**

Figure 12. Ocean bottom cable line 2 seismograms.

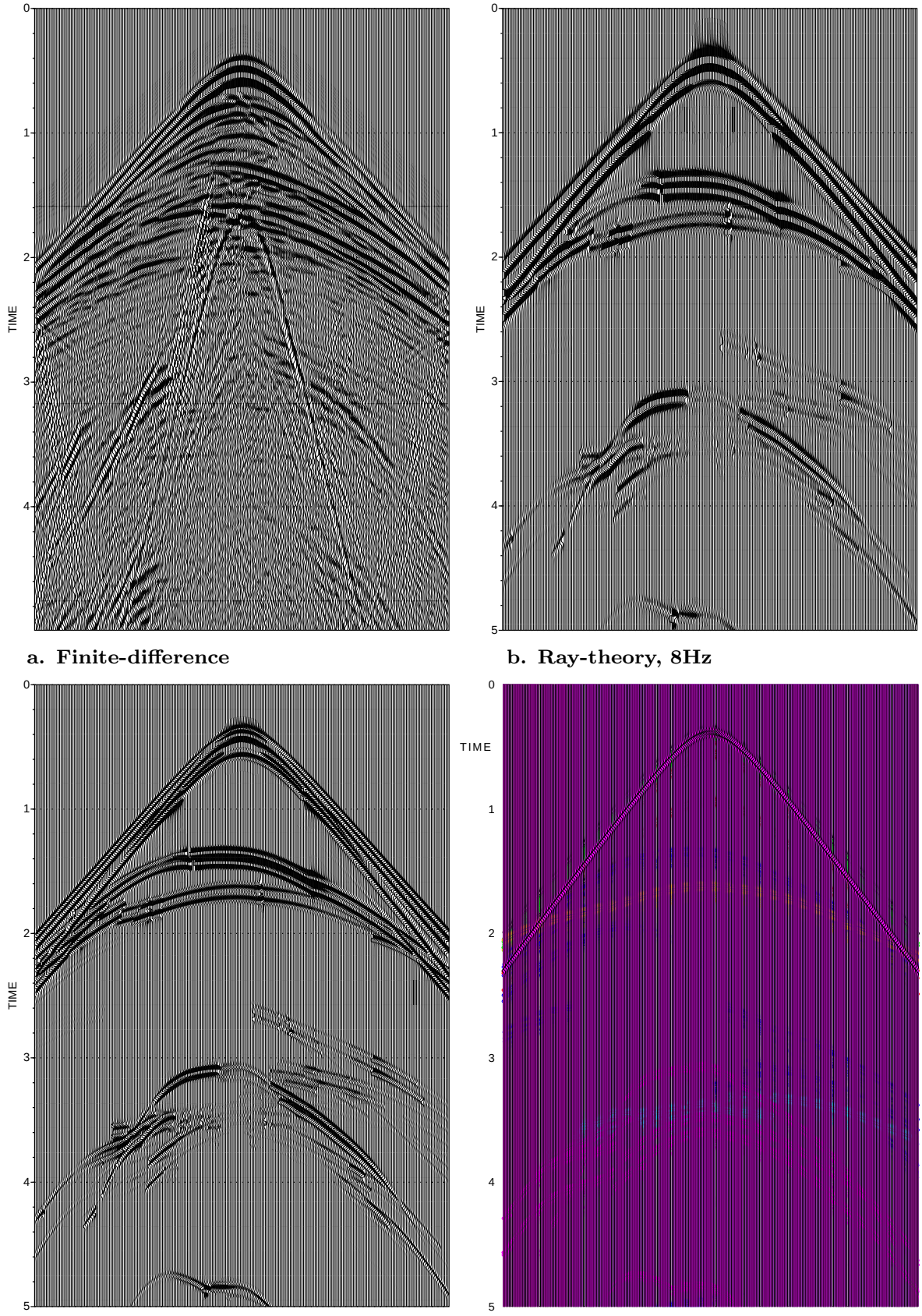

a. Finite-difference **b. Ray-theory, 8Hz**

c. Ray-theory, 15Hz **d. Ray-theory, individual waves, 15Hz**

Figure 13. Ocean bottom cable line 3 seismograms.

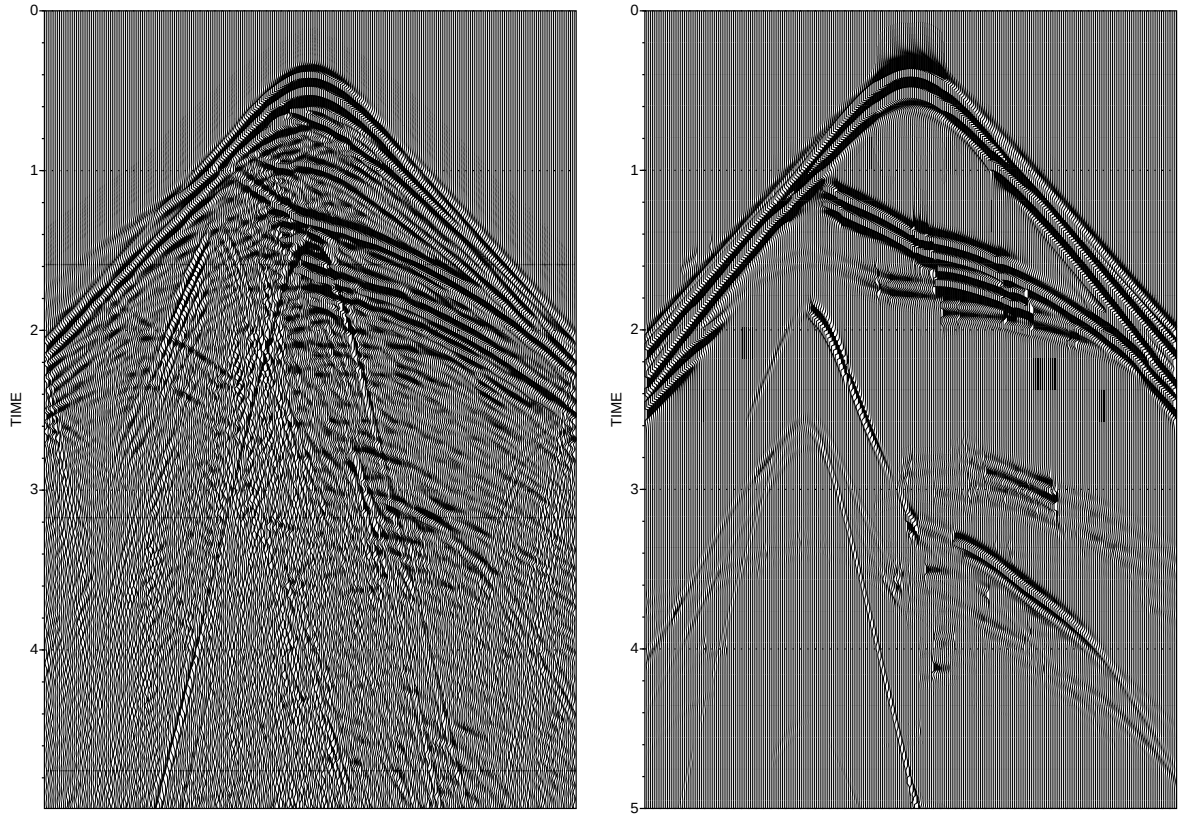

a. Finite-difference **b. Ray-theory, 8Hz**

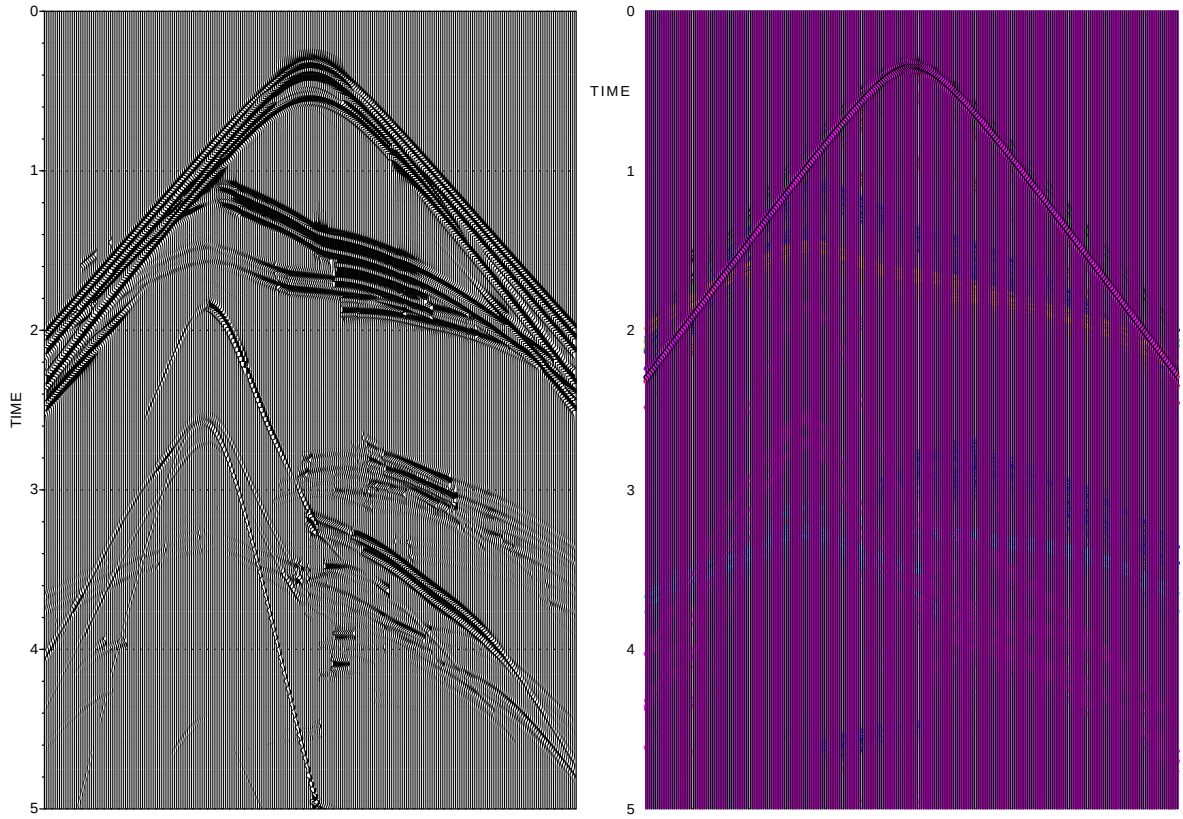

c. Ray-theory, 15Hz **d. Ray-theory, individual waves, 15Hz**

Figure 14. Ocean bottom cable line 4 seismograms.

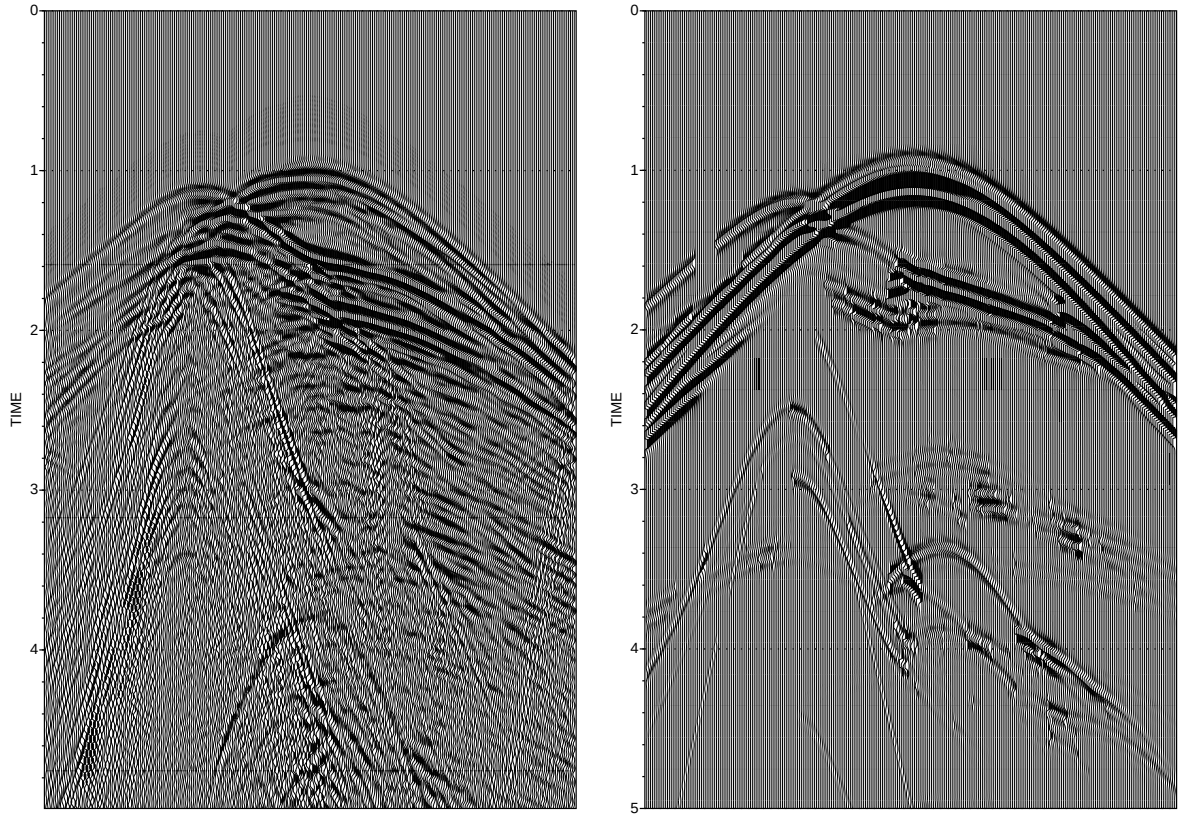

a. Finite-difference

b. Ray-theory, 8Hz

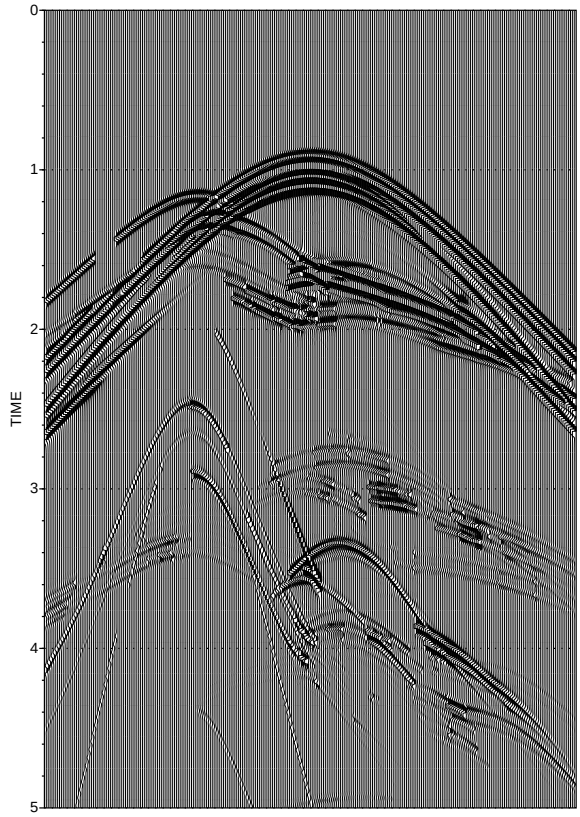

c. Ray-theory, 15Hz

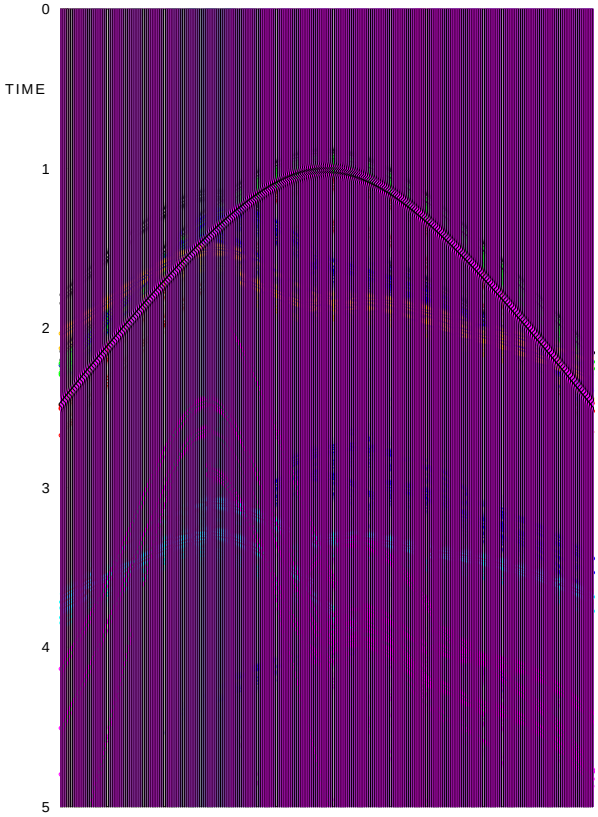

d. Ray-theory, individual waves, 15Hz

Figure 15. Ocean bottom cable line 5 seismograms.

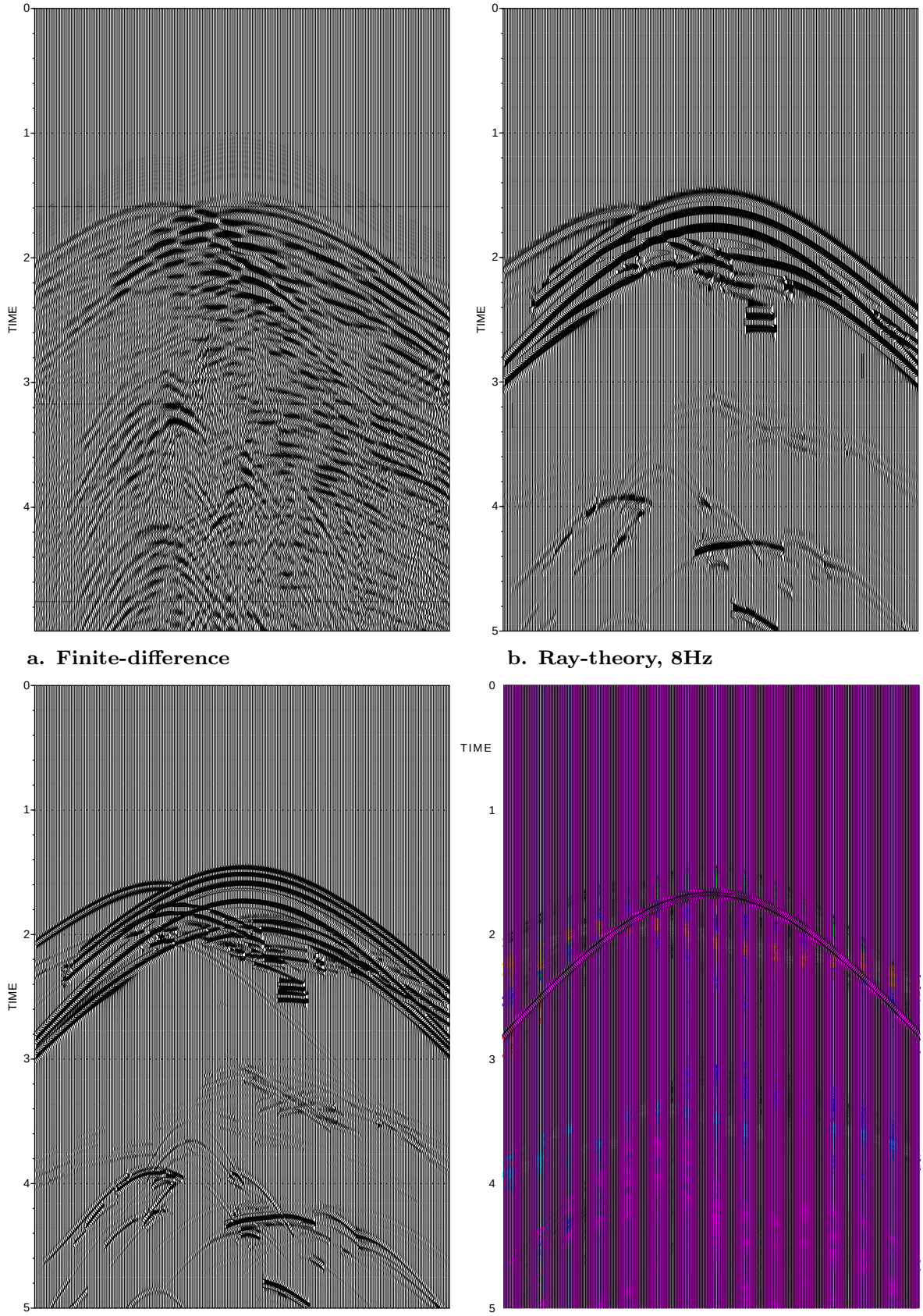

a. Finite-difference **b. Ray-theory, 8Hz**

c. Ray-theory, 15Hz **d. Ray-theory, individual waves, 15Hz**

Figure 16. Ocean bottom cable line 6 seismograms.

Acknowledgments

The author thanks to Luděk Klimeš for valuable comments and recommendations concerning this paper.

The research has been supported by the Grant Agency of the Czech Republic under Contracts 205/01/D097 and 205/04/1104, by the Grant Agency of the Charles University under Contract 375/2004/B-GEO/MFF and by the members of the consortium "Seismic Waves in Complex 3-D Structures" (see "http://seis.karlov.mff.cuni.cz").

References

Aminzadeh, F., Brac, J., Kunz, T. (1997): 3-D Salt and Overthrust Models, SEG/EAGE 3-D Modeling Series No.1. Soc. Explor. Geophysicists, Tulsa.

Bucha, V. (2001): Displaying 3-D seismic models through the VRML and GOCAD. In: Seismic Waves in Complex 3-D Structures, Report 11, pp. 337-355, Dep. Geophys., Charles Univ., Prague.

Bucha, V., Bulant, P. (eds.) (2005): SW3D-CD-9. In: Seismic Waves in Complex 3-D Structures, Report 15, pp. xxx, Dep. Geophys., Charles Univ., Prague.

Bulant, P. (2001): Sobolev scalar products in the construction of velocity models - application to model Hess, to SEG/EAGE Salt Model, and to model Pluto 1.5. In: Seismic Waves in Complex 3-D Structures, Report 11, pp. 133-159, Dep. Geophys., Charles Univ., Prague.

Bulant, P. (2002): Sobolev scalar products in the construction of velocity models: Application to model Hess and to SEG/EAGE Salt Model. Pure appl. Geophys., 159, pp. 1487–1506.

Bulant, P. (2003): Constructing the SEG/EAGE 3-D Salt Model for ray tracing using Sobolev scalar products. In: Seismic Waves in Complex 3-D Structures, Report 13, pp. 17-33, Dep. Geophys., Charles Univ., Prague.

Bulant, P. & Klimeš, L. (1998): Computations in the model composed during the 1998 consortium meeting. In: Seismic Waves in Complex 3-D Structures, Report 7, pp. 33–56, Dep. Geophys., Charles Univ., Prague.

Cohen, J.K. & Stockwell, Jr.J.W. (2004): CWP/SU: Seismic Un*x Release No. 38: a free package for seismic research and processing, Center for Wave Phenomena, Colorado School of Mines.

House, S., Larsen, S., Bednar, J.B. (2000): 3-D elastic numerical modeling of a complex salt structure. Exp. Abstr., Soc. Expl. Geophys. 70th Ann. Meet., pp. 2201-2204.

House, S., Larsen, S., Hoelting, C., Marfurt, K., Wiley, R. (2004): Next-Generation Seismic Modeling and Imaging project: summary of elastic modeling results. Exp. Abstr., Soc. Expl. Geophys. 74th Ann. Meet., pp. 2201-2204.